

Complex edge effects in zigzag graphene nanoribbons due to hydrogen loading

Sumanta Bhandary, Olle Eriksson, and Biplab Sanyal*

*Department of Physics and Astronomy,
Uppsala University, Box 516, 751 20 Uppsala, Sweden*

Mikhail I. Katsnelson

*Radboud University Nijmegen, Institute for Molecules and Materials,
Heyendaalseweg 135, 6525 AJ Nijmegen, The Netherlands*

(Dated: June 1, 2010)

Abstract

We have performed density functional calculations as well as employed a tight-binding theory, to study the effect of passivation of zigzag graphene nanoribbons (ZGNR) by Hydrogen. We show that each edge C atom bonded with 2 H atoms open up a gap and destroys magnetism for small widths of the nanoribbon. However, a re-entrant magnetism accompanied by a metallic electronic structure is observed from 8 rows and thicker nanoribbons. The electronic structure and magnetic state are quite complex for this type of termination, with sp^3 bonded edge atoms being non-magnetic, whereas the nearest neighboring atoms are metallic and magnetic. We have also evaluated the phase stability of several thicknesses of ZGNR, and demonstrate that sp^3 bonded edge atoms, with 2 H atoms at the edge, should be stable at temperatures and pressures which are reachable in a laboratory environment.

PACS numbers: 73.22.Pr, 75.70.Ak, 73.20.Hb, 81.05.U-

I. INTRODUCTION

The physical and chemical properties of graphene have lately been studied intensely.²⁻⁷ One of the reasons for this is the high electron mobility of this newly discovered material and the potential for scaling electronics devices to true nano-sizes. Hence this novel material holds exciting promises for applications in micro-electronics. For such applications, the possibility to create a band gap is important, and chemical functionalization have indeed been reported where the electronic properties were modified.⁸⁻¹³ Another avenue towards realizing this is through geometrical confinement, such as that provided by graphene nano-ribbons.

Nanoribbons of graphene, especially the zigzag edge terminated ones, have recently been under focus, both from experimental and theoretical studies. For instance, the possibility of breaking spin-degeneracy¹⁴ was shown, at least as given by first principles theoretical calculations. In this work an anti-ferromagnetic state across the nano-ribbon was found to have the lowest energy, with a resulting small gap opening up at the Fermi level. Furthermore, the mobility of atoms at the edge was studied experimentally in Ref. 15, where an edge-reconstruction was shown to be driven by Joule heating. Also, the dynamics of atoms at the edges of carbon nano-ribbons was investigated in Ref. 16 where, in addition, theoretical modeling based on kinetic Monte Carlo simulations were presented. These studies show that the coupling between geometry and electronic structure, and even magnetism, is strong in carbon nano-ribbons. It is important to note that recently the edge structure of zigzag graphene nanoribbon (ZGNR) was questioned, and instead theoretical and experimental evidence for a reconstructed edge geometry were reported, with alternating pentagons and heptagons at the edge, in a geometry called the reczag structure.^{17,18}

In graphene the C atoms are sp^2 bonded. Hence, an edge atom would have dangling bonds, which under any realistic circumstances would be saturated by an atom or molecular species. In order to make the theoretical modeling more realistic, a termination of the edge C atoms with one or two hydrogen atoms per carbon atom has been considered.^{19,20} In both these works the Gibbs energy was calculated as a function of, among other things, the temperature and pressure of the reference state of the H atoms, i.e. an H_2 gas. The edge termination of one H atom per C atom continues the sp^2 bonding of the graphene bulk, with a resulting planar geometry. This is normally referred to as 1H termination. The alternative

termination, with two H atoms per edge carbon atom provides a tetrahedral geometry of the C edge atoms, with sp^3 -bonding for the edge atoms. This termination is referred to as 2H termination and the stability of the 1H and 2H terminations can be calculated as a function of pressure and temperature of the reference state of the H atoms.

The magnetic properties of 1H terminated graphene have been studied theoretically to a large extent, and it is found that a spin-polarized solution gives a lower total energy compared to a spin-degenerate calculation. The magnetic properties of 2H terminated ZGNR have also been studied, and are found to be quite exotic, with the very outermost C atoms being spin-degenerate and having a gap of the electronic structure. The nearest neighboring C atoms have however a spin-polarized solution, as shown by tight-binding theory^{22,23} and first principles calculations of an 8 layer ZGNR.²⁴ Here we extend these studies to investigate various thicknesses of the ZGNR, and the stability, electronic structure and magnetic properties of 1H and 2H terminated ZGNR.

The paper is organized as the following. In section II, we have discussed the computational details used in this study followed by the results and discussions in section III. We have shown a model calculation in the support of our ab initio results in section IV followed by the conclusions.

II. COMPUTATIONAL DETAILS

First principles density functional calculations have been performed using the Quantum Espresso code²⁵ using plane wave basis sets and pseudopotentials. The exchange correlation potential has been approximated by using PBE functional²⁶ in the generalized gradient approximation (GGA). We have tested the convergence with respect to the basis-set cutoff energy and a value of 80 Ry. has been considered for all results shown in this paper. A 80x1x1 k-points set has been used for the one dimensional Brillouin zone. Structural optimizations have been done by minimizing the Hellmann-Feynman forces on each atom with a tolerance of 0.001 Ry./a.u. We have relaxed the structures with basis set cutoff energy value of 60 Ry. and one dimensional k-point mesh of 60x1x1. These parameters give very similar results as the ones calculated with 80 Ry. cutoff energy and 80x1x1 k-point mesh. For all cases, spin-polarized calculations were performed. Different widths (3 to 20 rows) of ZGNRs have been considered in our calculations. The computational unit cell has been chosen to be 20

Å long in the direction perpendicular to ZGNR plane and at least 15 Å along the y direction while the nanoribbon is infinite in the x-direction.

III. RESULTS

The dangling bonds of edge C atoms of nanoribbons are extremely reactive and need to be saturated, if one has the ambition to model a realistic situation. There are several possibilities of edge termination. We concentrate on H termination at the edges as this seems to be one of the most stable configurations owing to its simple planar structure. Although the structure remains planar, C atoms rearrange themselves on relaxation and reach a bond-distance close to 1.42 Å (which is the bulk graphene bond length) in the middle of the ribbon. We carried out calculations for 1H termination with different widths, from 3 rows up to 20 rows. We observe that 1H terminated ZGNR is metallic and spin-polarized with an average moment of $0.25 \mu_B/\text{C atom}$ in agreement with previous DFT calculations²⁷. We note however that to date, there is no firm experimental evidence of magnetism in GNRs. This could be due to that the edge atoms undergo a structural distortion, which quenches magnetism¹⁷, or due to the one-dimensional geometry of the spin-polarized atoms, which according to the Mermin-Wagner theorem should not order at any finite temperature. At finite temperatures, instead of ferromagnetism, a superparamagnetism should appear, with an enhancement factor for the magnetic susceptibility, roughly, 8 at room temperature, according to the calculations²⁸. There is however another scenario, where the edge C atoms have all their bonds saturated, so that the absence of the lone pair electron results in a nonmagnetic state. The relevant situation is when two H atoms terminate a C atom. The chemical binding for this edge C atom is an sp^3 hybrid, with two C atoms and two H atoms as nearest neighbors. It is this termination we explore here, both in terms of the energetics, but also the electronic structure and magnetic properties.

For the termination of edges with 2 H atoms per C, the formation energies have been defined in two ways:

$$E_f^{(1)} = E(G2H) - [E(G1H) + E(H_2)]$$

$$E_f^{(2)} = E(G2H) - [E(G1H) + 2[E(H) + (B.E./H)_{exp}],$$

where $E(G2H)$ and $E(G1H)$ are the total energies for the zigzag graphene nanoribbons'

edges terminated with 1 H and 2 H atoms per edge, respectively. $E(H_2)$ and $E(H)$ are the calculated energies for a H_2 molecule and a H atom, respectively. $(B.E./H)_{exp}$ is the experimental binding energy per H atom of the H_2 molecule, and it amounts to 2.24 eV. Our calculated value is 2.27 eV, which is in very good agreement with the experimental one.

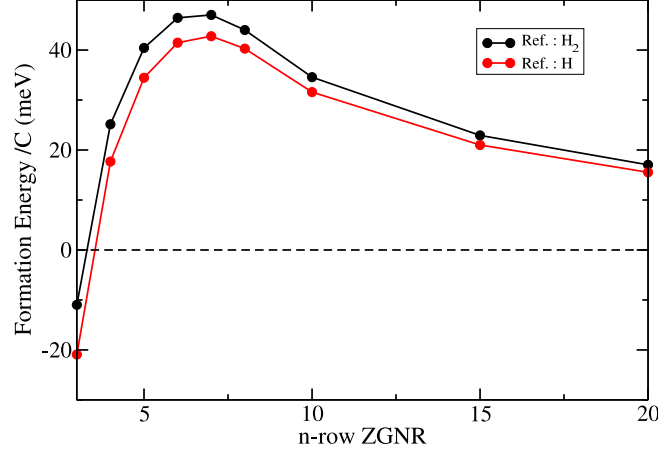


FIG. 1: (Color online) Calculated formation energies according to the equations shown in the text for different widths of nanoribbons. Ref.: H_2 and Ref.:H indicate the calculated values using the expressions for $E_f^{(1)}$ and $E_f^{(2)}$ respectively.

The formation energies are shown in Fig. 1 using the two equations presented above. These energies indicate that the formation of 2H terminated edges is probable. The formation energies tend to decrease with the increase in the width of the nanoribbon whereas for 3-rows ZGNR it is at T=0 K spontaneously formed. In order to investigate the influence of finite temperature/elevated gas pressure, we have evaluated the Gibbs free energy of the reference phase, the gas phase of the H atoms. Hence, we have calculated the Gibbs free energy as a function of the chemical potential of the hydrogen molecule, according to the following formula given by Wassmann *et al.*²⁰.

$$\begin{aligned}
G_{H_2} &= E_{H_2} - 2\mu_{H_2} \\
E_{H_2} &= E(G2H) - [E(G1H) + E(H_2)] \\
\mu_{H_2} &= H^0(T) - H^0(0) - TS^0(T) + k_B T \ln\left(\frac{P}{P_0}\right)
\end{aligned}$$

In the above equations, μ_{H_2} , H , S , P and k_B are the chemical potential, enthalpy, entropy,

pressure and Boltzmann constant respectively. The values for the entropies and enthalpies are taken from the tabular data presented in Ref. 21. P^0 is the reference pressure taken to be 0.1 bar according to the tabular data. $E(G2H)$, $E(G1H)$ and $E(H_2)$ have been defined above. The results are shown in Fig. 2 for 100 K and 300 K. One can observe the stability of the nanoribbons terminated with 2H at certain pressures indicated in the plots. The 20 rows-ZGNR requires lower pressure of the H_2 gas, compared to the 8-rows ZGNR, both for 100 K and 300 K case (the 2H terminated ZGNR is stable at negative values in the plot). As seen in the plots, the chemical pressure of molecular hydrogen required to stabilize a 2H terminated ZGNR is within the range of laboratory values.

With two H atoms terminating a C atom, the chemical bonds are now completely saturated, which results in a vanishing magnetic moment of this atom. In addition, we observe the appearance of distortions in the ZGNR plane. The sp^2 planar structure now becomes buckled, making a sp^3 like structure with an angle of 102° at the edge carbon. The C-C bond length increases at the edge (see Fig. 3) and this bond-stretching remains almost the same, for all widths of the ribbon. However, the inner bond-lengths have an oscillatory behavior as one traverses towards the center of the ribbon (Fig. 3). The C-C bond length of 1.42 Å in sp^2 bonded graphene is recovered in the middle of the ribbon. For the 20 rows nanoribbon, the bond-length reaches the ideal value in bulk graphene around the 15th bond from the edge. It is obvious that the edge sp^3 structure has a pronounced effect on smaller ribbons by perturbing the whole structure where as for wider ribbons, this perturbation dies out and we get a planar valley along with sp^3 distorted edge as seen in Fig.3. Besides the edge region with a CH_2 unit, the wider ribbons have similar features as in 1H terminated ribbons which are of planar sp^2 type throughout their structures.

Due to the formation of an sp^3 like structure at the edge and hence the appearance of an energy gap in the electronic spectrum, the 2H terminated ZGNR is non-magnetic. The density of states (DOS) for different widths of ZGNR with 2H edge termination are shown in Fig.4. One can clearly observe band gaps for 3 and 4-rows ZGNRs with values 2.1 eV and 2.08 eV, respectively. The band gaps decrease with an increase in the ribbon width up to 7 rows ZGNR. A semiconductor to metal transition happens for an 8 row ZGNR. We observe that the Fermi level cuts through a peak in the non-magnetic DOS (right-hand side of Fig. 4). The high value of the DOS at the Fermi level leads to an instability and hence a spin-polarized solution leads to a lower energy state. We have performed both non-spin

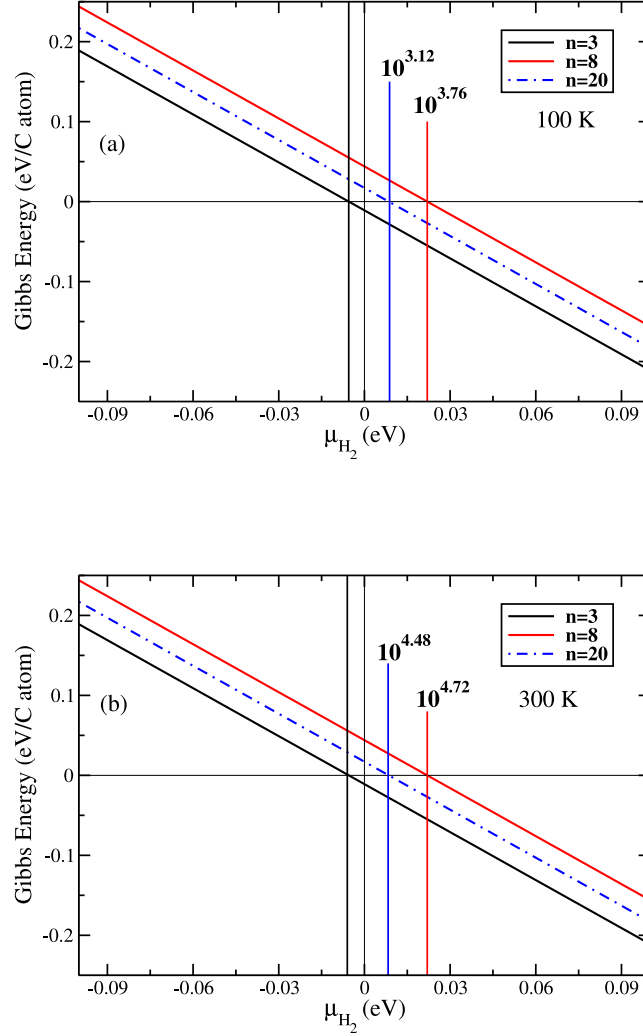


FIG. 2: (Color online) Calculated Gibbs formation energies for $n=3$, 8 and 20 thick ZGNR, at (a) 100 K and (b) 300 K as a function of chemical potential of hydrogen molecule according to the equations shown in the text. For the sake of clarity, the vertical bars are shown to indicate the corresponding chemical potentials for which the Gibbs free energies become negative. The numbers indicate the pressures in bar corresponding to the vertical bars.

polarized and spin-polarized calculations for system sizes ranging from 8 to 20 rows ZGNR. The results are presented in Table I where it is seen clearly that the ribbons have a magnetic ground state, which is also metallic. This re-entrant magnetism, which occurs despite the presence of 2H termination is an interesting observation which we will analyze in detail

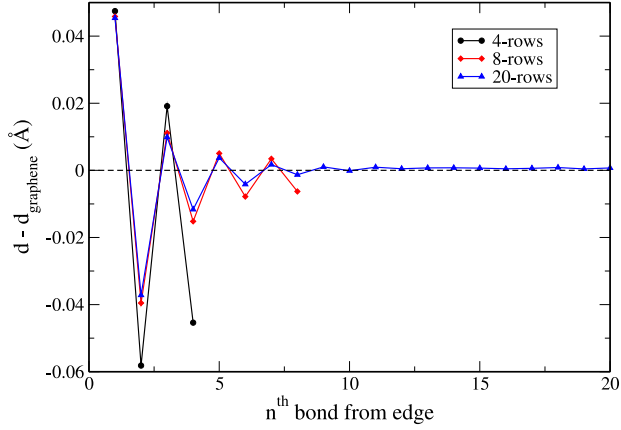


FIG. 3: (Color online) Calculated C-C bond lengths relative to an ideal 2D graphene layer (1.42 \AA) for different bonds from the edge towards the center of ZGNRs, with thickness 4, 8 and 20 rows.

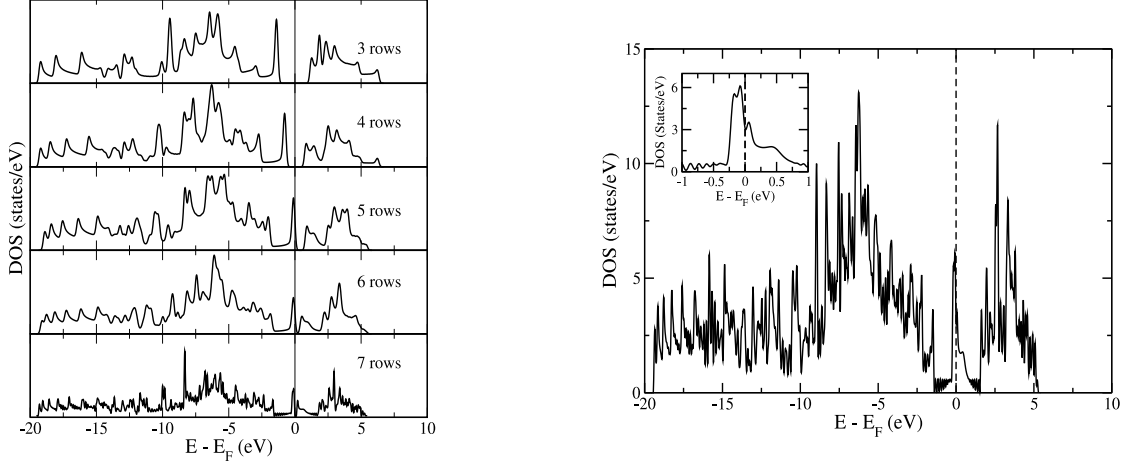


FIG. 4: (left) Calculated total DOS's of 2H edge terminated nanoribbons of various widths. (right) Total DOS of an 8 row ZGNR for a non-spin polarized calculation with (inset) expanded view of the DOS near the Fermi level.

below.

A detailed analysis of the magnetic structure shows that the second C atom from the edge carries most of the magnetic moment. This second C atom from the edge develops in a non-magnetic calculation a mid-gap state, due to the strong perturbation to the potential

TABLE I: Difference in total energies between the non-magnetic and ferromagnetic states (ΔE) and the corresponding magnetic moments in the ferromagnetic state. The energy differences and total magnetic moments are quoted for the unit cell whereas the edge moment is for one C atom at the edge.

width (rows)	ΔE (meV)	Total moment (μ_B)	Edge moment (μ_B)
8	1.63	1.04	0.34
10	5.3	1.23	0.38
15	4.9	1.29	0.39
20	3.81	1.3	0.39

its nearest neighboring C atom at the edge experiences. The strong perturbation of the edge C atom is an effect of the drastic difference in bonding and electronic structure of an sp^3 bonded atom, compared to an sp^2 bonded one. For this reason, the situation of the second C atom from the edge is quite similar to the edge atoms of 1H terminated ZGNR. The resulting sharp peak from the midgap state then drives the magnetic solution of these atoms. There is one important difference between the magnetism of the 1H terminated ZGNR and the 2H terminated ZGNR, in that geometrical distortions of the network of sp^3 bonded atoms are unlikely, and hence one does not expect Peierls-like structural distortions, which modify the electronic structure so that the sharp peak of the DOS at the Fermi level disappears.

Fig.5 depicts the projected DOSs of the atoms starting from the edge and going inwards for a 8-rows ZGNR. The edge atom experiences a gap in the DOS due to sp^3 bonding and in contrast, the DOS of the second carbon atom from the edge with a p_z orbital character has a sharp peak at the Fermi level giving rise to a spin-polarized ground state due to a Stoner instability. This alternative occurrence of a gap and a spin-polarized state for the neighboring carbon atoms persists for a certain distance from the edge, albeit with a decreasing magnitude as the center of the ribbon is approached. The two different behaviors of carbon atoms situated in different sublattices can be described by the analysis of mid-gap states through a tight-binding model, which we will present later on in the paper. An inspection of the band structure (Fig.5 (right)) reveals a crossing of spin-up and spin-down bands at the Fermi level as seen in the case for a 1H terminated ZGNR.

We have also calculated the electronic structures of the 2H terminated nanoribbons with

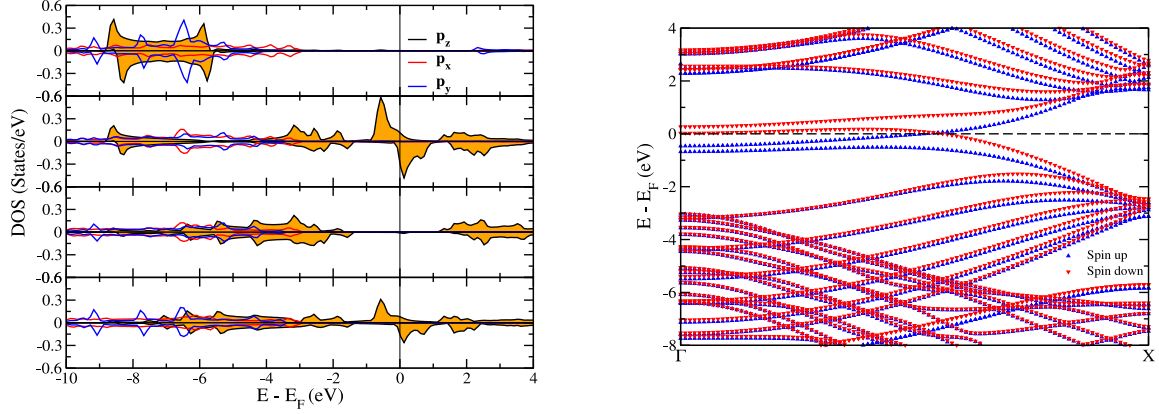


FIG. 5: (Color online) (left) Calculated DOS for 2H edge terminated 8-rows nanoribbon. (Right) Spin-polarized band structure for 2H edge terminated 8-rows zigzag nanoribbon. Both spin-up and spin-down bands are shown.

antiferromagnetic (AFM) spins across the ribbon. The AFM state is lower in energy than the ferromagnetic state as observed for 1H terminated ZGNRs. As a result, a gap opens up at the Fermi level. As we are mostly interested in the onset of local magnetism in the wide ribbons, since long range ordered moments in low dimensional systems is hindered by the Mermin-wagner theorem, we will not discuss further the AFM state but the FM one only.

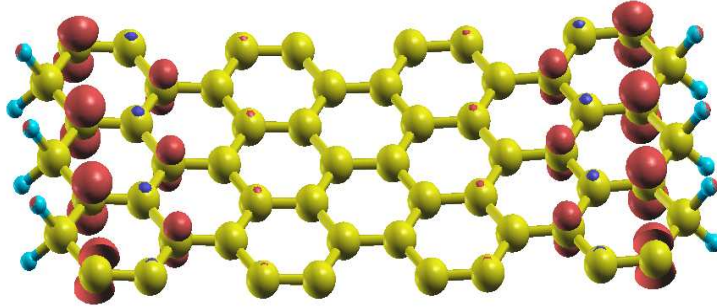


FIG. 6: (Color online) Isosurface plot of magnetization density of a 8-rows 2H terminated ZGNR.

In Fig.6, we show the magnetization density of an 8-rows ZGNR with 2H termination. In accordance to Fig.5, we observe the existence of a magnetization density which starts at the nearest C neighbor to the sp^3 bonded C-edge atom. We also note from the figure that only alternative carbon atoms close to the edge of the nanoribbon have a magnetic moment and a non-zero magnetization density.

IV. MODEL CALCULATIONS

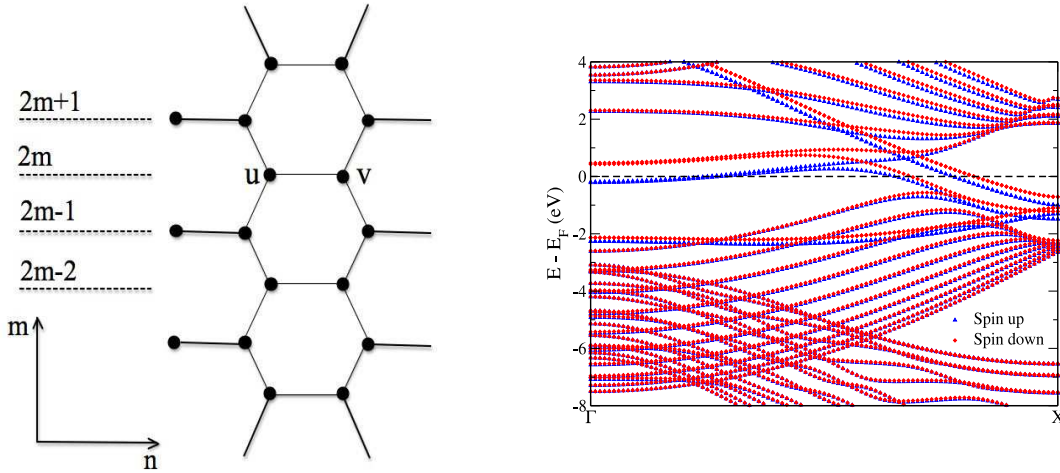


FIG. 7: (Color online) (left) A schematic diagram for the model theory. (right) Spin-polarized band structure for the carbon-terminated structure shown at the left panel. Both spin-up and spin-down bands are shown.

The first principles results presented here seem to be, at a first look, counterintuitive. Indeed, two hydrogen atoms attached to carbon at the zigzag edge take away all unpaired electrons, thus, naively speaking, there is no reason to expect that the system should become magnetic. In order to analyze the first-principles calculations of the previous section, we have carried out analytic calculations with a tight-binding model. A schematic diagram of the model is shown in Fig.7. In this model we introduce a simple tight-binding Hamiltonian of the p_z orbitals for semi-infinite graphene, presented in Fig.7. We assume that the main effect of the double hydrogenation is a local gap opening which can be approximately taken into account within the model where the hydrogenated carbon atom is not available for the itinerant π -bonded electrons. If we would remove all these atoms, we would obtain

a carbon-terminated structure shown in Fig.7 (originally, the hydrogenated atoms were in even rows). The extreme left carbon atoms in the model are in reality connected with the next left row of double hydrogenated carbon atoms, but, due to local gap opening at these atoms, within the gap the double hydrogenated atoms are unavailable for electrons. Our model assumption (just to interpret the ab initio results presented above) is that the double hydrogenated carbon atoms are unavailable for electrons at *any* energies and thus can be simply removed.

In the tight-binding model with the nearest-neighbor hopping only (the strength of the hopping parameter is put equal to 1 in our model) the two-component wave function (u, v) and the single-electron energy E can be found from the set of equations

$$\begin{aligned}
Eu(2m, n) &= v(2m, n) + v(2m + 1, n - 1) + v(2m - 1, n - 1) \\
Ev(2m, n) &= u(2m, n) + u(2m + 1, n) + v(2m - 1, n) \\
Eu(2m + 1, n) &= v(2m + 1, n) + v(2m + 2, n) + v(2m, n) \\
Ev(2m + 1, n) &= u(2m + 1, n) + u(2m + 1, n + 1) + u(2m - 1, n + 1)
\end{aligned} \tag{1}$$

where $n = 1, 2, \dots$ labels atoms in the direction perpendicular to the edge. For the terminating atoms ($n = 0$) one has, instead,

$$\begin{aligned}
Eu(2m + 1, 0) &= v(2m + 1, 0) \\
Ev(2m + 1, 0) &= u(2m + 1, 0) + u(2m + 2, 1) + u(2m, 1)
\end{aligned} \tag{2}$$

Due to translational invariance in the m -direction one can try the solutions as

$$\begin{aligned}
u(2m + 1, n) &= u_1(n) e^{i\xi(2m+1)}, \\
v(2m + 1, n) &= e^{i\xi(2m+1)}, \\
u(2m, n) &= u_2(n) e^{2i\xi m}, \\
v(2m, n) &= v_2(n) e^{2i\xi m}
\end{aligned} \tag{3}$$

One can see immediately that Eqs. 1-3 have a solution with $E = 0$, $v_1 = v_2 = 0$ and

$$\begin{aligned}
u_1(n) &= \frac{1}{(2 \cos \xi)^{2n}} u_1(0), \\
u_2(n) &= -(2 \cos \xi) u_1(n).
\end{aligned} \tag{4}$$

which corresponds to the surface states at $2|\cos\xi| > 1$, otherwise, we have nonphysical solutions growing to the bulk. These surface states belong to only one sublattice (u) and give contribution to the density of states $\frac{2}{3}\delta(E)$ per two lines of carbon atoms (the factor $2/3$ is just a fraction of allowed values of ξ). When taking into account exchange interactions between electrons, this delta-functional peak immediately leads to the Stoner instability and, thus, to ferromagnetism.

Eqs.(1)-(3) can be solved analytically for finite E as well, but the solutions are rather cumbersome. Instead of presenting them here, we show in Fig.7 the results of first-principles calculations for the carbon-only structure shown in the left panel of Fig.7. Indeed, we have midgap states in non-spin-polarized case and ferromagnetism when system is allowed to have spin polarization. Our calculated total energies reveal that the spin-polarized solution has a lower energy compared to a non-spin polarized one by 34.51 meV. The spin-polarized band structure shown in Fig.5 has 2 spin-up and 2 spin down bands crossing the Fermi level in contrast to the crossing of 1 spin-up and 1 spin-down bands. The analysis of the local magnetic moments show that the edge C atom (one replacing H) has $0.3 \mu_B$ and the moments decrease fast for the same sublattice C atom. An opposite and much weaker spin-polarization is observed for the C atom connected to the edge C atom and the same sublattice-behavior is observed in this case too. For thick enough ribbons, these surface states leads to the ferromagnetism which explains our first principles results. However, if the ribbon is very thin, the electron tunneling from one edge of the ribbon to another one is strong enough to split the midgap state which suppresses the spin polarization.

V. CONCLUSION

We have studied graphene nanoribbons with zigzag edges terminated with different hydrogen concentrations to observe how the modification along with quantum confinement and edge effects bring changes to the electronic and magnetic properties. ZGNR with one H atom termination per edge C atom is magnetic and an antiferromagnetic coupling between edges stabilizes the structure resulting a band gap which can be controlled by varying the width of nanoribbon. Interesting features appear when the ZGNR is terminated by 2 H atoms leading for narrow widths of the ZGNR to a non-magnetic semiconducting system with an energy gap that decreases with the increase of width. For sufficiently large widths

of the ZGNR, the 2 H terminated system becomes a metallic magnet if antiferromagnetism across the ZGNR can be ordered ferromagnetically by an applied magnetic field. The strong sensitivity of the metallic character with respect to an applied field is an interesting fact that could be relevant for sensor application and spintronics. The electronic structure and magnetic state are quite complex for this type of termination, with the sp^3 bonded edge atoms being non-magnetic with a gap in the electronic structure, whereas the nearest neighboring atoms are metallic and magnetic. As one proceeds further in to the center of the ZGNR this trend holds, with every row being non-magnetic and the alternating ones having a magnetic moment. The results from ab initio theory have been supported by a tight-binding model, which demonstrates the presence of midgap states as the driving force for the magnetic state. We have also evaluated the phase stability of several thicknesses of ZGNR, and demonstrate that sp^3 bonded edge atoms, with 2 H atoms at the edge, should be stable at temperatures and pressures which are reachable in a laboratory environment.

VI. ACKNOWLEDGEMENT

We gratefully acknowledge financial support from the Swedish Research Council (VR), Swedish Foundation for Strategic Research (SSF), Göran Gustafsson Foundation, Carl Tryggers Foundation, STINT, the EU-India FP-7 collaboration under MONAMI, and a KOF grant from Uppsala University. O.E. is grateful to the ERC for support. We also acknowledge Swedish National Infrastructure for Computing (SNIC) for the allocation of time in high performance supercomputers. MIK acknowledges a support from Stichting voor Fundamenteel Onderzoek der Materie (FOM), the Netherlands.

* Electronic mail: Biplab.Sanyal@fysik.uu.se

² A.K. Geim and K.S. Novoselov, *Nature Mater.* **6**, 183 (2007).

³ M.I. Katsnelson, *Mater. Today* **10**, 20 (2007).

⁴ A.H. Castro Neto, F. Guinea, N.M. Peres, K.S. Novoselov, and A.K. Geim, *Rev. Mod. Phys.* **81**, 109 (2009).

⁵ A.K. Geim, *Science* **324**, 1530 (2009).

⁶ S. Das Sarma, S. Adam, E.H. Hwang, and E. Rossi, arXiv:1003.4731.

- ⁷ M.A.H. Vozmediano, M.I. Katsnelson, and F. guinea, arXiv:1003.5179.
- ⁸ V. A. Coleman, R. Knut, O. Karis, H. Grennberg, U. Jansson, R. Quinlan, B. C. Holloway, B. Sanyal, O. Eriksson, J. Phys. D: Appl. Phys. **41**, 062001 (2008).
- ⁹ B. Sanyal, O. Eriksson, U. Jansson and H. Grennberg, Phys. Rev. B **79**, 113409 (2009).
- ¹⁰ S. H. M. Jafri et al., J. Phys. D: Appl. Phys. **43**, 045404 (2010).
- ¹¹ J. O. Sofo, A. S. Chaudhari, and G. D. Barber, Phys. Rev. B **75**, 153401 (2007).
- ¹² D. C. Elias, et al. Science **323**, 610 (2009).
- ¹³ S. Lebegue, et al. Phys. Rev. B **79**, 245117 (2009).
- ¹⁴ Y.W. Son, S. Louie, and M.L. Cohen, Nature **444** 347 (2006).
- ¹⁵ X. Jia et al., Science **323**, 1701 (2009)
- ¹⁶ C. Girit et al. Science **323**, 1705 (2009).
- ¹⁷ P. Koskinen, S. Malola, and H. Häkkinen, Phys. Rev. Lett. **101**, 115502 (2008).
- ¹⁸ P. Koskinen, S. Malola, and H. Häkkinen, Phys. Rev. B **80**, 073401 (2009).
- ¹⁹ C. K. Gan and D. J. Srolovitz, Phys. Rev. B **81**, 125445 (2010).
- ²⁰ T. Wassmann, A. P. Seitsonen, A. M. Saitta, M. Lazzeri, and F. Mauri, Phys. Rev. Lett. **101**, 096402 (2008).
- ²¹ M. W. Chase, Jr., J. Phys. Chem. Ref. Data, Monog. **9** (1998).
- ²² K. Kusakabe and M. Maruyama, Phys. Rev. B **67**, 092406 (2003).
- ²³ H. Lee, Y.-W. Son, N. Park, S. Han, and J. Yu, Phys. Rev. B **72**, 174431 (2005).
- ²⁴ B. Xu, J. Yin, Y. D. Xia, X. G. Wan, K. Jiang, and Z. G. Liu, Appl. Phys. Lett. **96**, 163102 (2010).
- ²⁵ P. Giannozzi et al., *www.quantum-espresso.org*.
- ²⁶ J. P. Perdew, K. Burke and M. Ernzerhof, Phys. Rev. Lett. **77**, 3865 (1996).
- ²⁷ Y. -W. Son, M. L. Cohen and S. G. Louie, Phys. Rev. Lett. **97**, 216803 (2006).
- ²⁸ O.V. Yazyev and M.I. Katsnelson, Phys. Rev. Lett. **100**, 047209 (2008).